Int. J. Therm. Sci. (2000) 39, 225–235

S1290-0729(00)00241-6/FLA

Flow boiling heat transfer characteristics of wide-boiling mixtures

Matthias Wettermann[1], Dieter Steiner*

Institut für Thermische Verfahrenstechnik, Universität Karlsruhe (TH), Kaiserstr. 12, D-76128 Karlsruhe, Germany

(Received 30 May 1999, accepted 2 August 1999)

Dedicated to Prof. Dr.-Ing. Dr. h.c. mult. E.-U. Schlünder on the occasion of his 70th birthday

Abstract — Heat transfer coefficients in horizontal flow boiling of the wide-boiling binary mixture of $C_2F_6/C_2H_2F_4$ and of the ternary mixture $C_2F_6/SF_6/C_2H_2F_4$ are measured. The experiments are carried out with the condition of uniform inner wall temperature at the tube perimeter. Results of the two boiling regions—forced convective evaporation and nucleate boiling—are obtained. In the forced convective evaporation region the results are predicted best using a pure fluid correlation which takes mixture properties into account. In the nucleate flow boiling region a degradation of the heat transfer coefficients occurs. This degradation has to be predicted with a suitable mass transfer controlled model, based on the ideal heat transfer coefficient, provided that a certain heat flux limit is not exceeded. In the region of high heat fluxes an "effective" heat transfer coefficient, based on local total vaporization, is more suitable than the previously cited ideal heat transfer coefficient. © 2000 Éditions scientifiques et médicales Elsevier SAS

flow boiling / heat transfer / degradation / mixture / high heat fluxes

Nomenclature

B_0	parameter in equation (9)	
c_p	specific heat capacity	$J \cdot kg^{-1} \cdot K^{-1}$
g	gravitational acceleration	$m \cdot s^{-2}$
$\Delta\tilde{h}_v$	latent enthalpy of vaporization of mixture	$J \cdot kmol^{-1}$
$\dot{m}$	mass velocity	$kg \cdot m^{-2} \cdot s^{-1}$
p	pressure	Pa
p_r	reduced pressure ($p/p_{c,m}$)	
$\dot{q}$	heat flux	$W \cdot m^{-2}$
T	temperature	K
$\dot{x}$	vapour mass fraction (quality)	
$\tilde{x}_i$	mole fraction of component i	
z	coordinate in main flow direction	m

Greek symbols

α	heat transfer coefficient	$W \cdot m^{-2} \cdot K^{-1}$
β	mass transfer coefficient	$m \cdot s^{-1}$
ρ	density	$kg \cdot m^{-3}$
$\tilde{\rho}$	molar density	$kmol \cdot m^{-3}$
σ	surface tension	$N \cdot m^{-1}$
φ	angle at circumference	

Subscripts

B	boundary
bp	boiling range
c	critical condition
ce	convective evaporation
c, m	critical condition mixture
cr	critical heat flux
cv	convective vaporization
d	dew point
G	vapour
G0	total mass velocity assumed as vapour
I	interphase
id	ideal
L	liquid
L0	total mass velocity assumed as liquid
max	maximum
min	minimum
nb	nucleate boiling
nbf	nucleate flow boiling
ONB	onset of nucleate boiling
s	saturation point

---

* Correspondence and reprints.
dieter.steiner@ciw.uni-karlsruhe.de

[1] Present address: Seeger GmbH, Postbox 160, D-73651 Plüderhausen, Germany.

w wall
1 more volatile component

1. INTRODUCTION

Process industry needs reboilers and evaporators with vaporization of mixtures inside tubes. Current trends in more efficient energy utilisation and the use of costly materials (e.g., titanium) are the basis for a better prediction of heat transfer. Compared with pool boiling, only a limited number of results on convective vaporization inside tubes are available. Additionally, the results are quite inconsistent with one another.

The mixture effect of hydrocarbons on the heat transfer coefficient was taken into account by Palen and Small [1] as a function of boiling range, ΔT_{bp} (dew point temperature minus bubble point temperature). Aqueous mixtures of iso-propanol, n-propanol and glycerol were tested by Calus et al. [2] in a vertical tube. The effective temperature difference is used in their correlation which incorporates the diffusional resistance of the more volatile component in the liquid film. The evaporation of ethanol/water mixtures in a heated vertical tube was studied experimentally by Shock [3]. The experiments were carried out in the subcooled and low quality region. Shock concluded that the mass transfer in the liquid film is negligible and that the vapour phase resistance can often be neglected. Zizyukin and Aérov [4] measured flow boiling of binary and ternary hydrocarbons in a horizontal tube. These data could be correlated with the Lockhart–Martinelli parameter, X_{tt}, and the phase transformation parameter, K_{p}, only.

Forced convective heat transfer data for aqueous mixtures with ethylene glycol (high Prandtl number) are experimentally determined by Bennett and Chen [5] in a vertical tube. They extended the widely quoted Chen correlation for pure fluids with a mixture factor for the convective and the nucleate boiling contribution to the heat transfer coefficient. Both factors are based on the mass transfer effect during vaporization. Toral et al. [6] measured local heat transfer coefficients for ethanol/cyclohexane mixtures in a vertical tube for upward flow. They found that the boiling curves of mixtures (excluding their azeotropes) have much smaller slopes than the pure components. Experimental data of flow boiling of $CCl_2F_2/CClF_3$ mixtures in a horizontal tube are presented by Jain and Dhar [7]. They showed that the reduction of the heat transfer coefficient in the dominant convective evaporation region is rather small, while in the nucleate flow boiling region the reduction is quite significant. However, the correlations include a mixture correction factor for each of the convective and nucleate flow boiling regions.

Radermacher et al. [8–11] used a horizontal test section to determine perimeter-averaged heat transfer coefficients of various refrigerant mixtures. They tested the heat transfer of mixtures with CH_3CHF_2/CF_3Br reported in [8, 9] and $CHClF_2/C_2Cl_2F_4$ reported in [10]. The results indicate that the majority of the data belong to the convective evaporation region. Additionally, Jung et al. [11] report experimental data of CCl_2F_2/CH_3CHF_2 mixtures. The given correlation of an additive type, referred to as Chen-type [12], was corrected by a mixture factor for both regions, the convective and the nucleate boiling, respectively.

In 1989 Thome [13] proposed a Chen-type correlation method. He used the mass transfer based equation of Schlünder [14] as nucleate boiling contribution to the heat transfer, however modified with the boiling range temperature, ΔT_{bp}, and compared this and other mixture boiling correlations with the data given by Toral et al. [6]. Flow boiling heat transfer of binary mixtures of $CHClF_2/C_2Cl_2F_4$ was experimentally investigated in a horizontal tube by Hihara and Saito [15]. They used a correlation where the heat transfer coefficient is a function of the Lockhart–Martinelli parameter, X_{tt}, and the boiling number, Bo. Unfortunately, the required coefficients depend on the composition. Recently, these authors [16] measured flow boiling heat transfer with a ternary mixture $CH_2F_2/CHF_2CF_3/C_2H_2F_4$ and suggested an additive type correlation. Experimentally determined data of the mixture $CHClF_2/C_2Cl_2F_4$ in a horizontal tube with internal spiral grooves are given by Takamatsu et al. [17]. Again an empirical fit using X_{tt} and Bo is used to predict the heat transfer with composition dependent coefficients. Celata et al. [18, 19] measured the heat transfer coefficient of the binary mixture of $CCl_2F_2/C_2Cl_2F_4$ in a vertical tube. All data belong to the inlet subcooled fluid condition and show a remarkable reduction of mixture heat transfer coefficients compared with that of the pure fluids.

Recently, Fujita and Tsutsui [20] used a vertical tube to measure the boiling heat transfer of binary mixtures of $CF_3CH_2F/CHCl_2CF_3$. The authors show that the reduction of mixture heat transfer coefficients depends on the composition and increases with the heat flux. Mixtures of $CHClF_2/C_2H_3ClF_2$ and of propane/n-butane are used by Melin and Vamling [21] experimentally to determine heat transfer coefficients in a horizontal tube. The authors observed the decrease in heat transfer of mixtures with composition, where the largest decrease is found for 50 %/50 % mixtures. Additionally, a strong correlation between the boiling range, ΔT_{bp}, and the decrease in heat transfer was observed. A ternary mixture with small differences in boiling temperatures (CH_2F_2/C_2HF_5/$C_2H_2F_4$) were tested by Aprea et al. [22]. The average heat transfer coefficients of the evaporator are predicted with pure fluid correlations only.

In the previously discussed reports the local composition of the fluid was not measured, except in the report of Calus et al. [2]. Instead, the initially-charged or overall composition, measured at any point of the test apparatus, was used in the evaluation of the fluid temperature and as a basis of the effect of composition on the heat transfer. In many reports, the fluid temperature has been evaluated with equations of state assuming thermodynamic equilibrium. An estimation of data accuracy shows a remarkable error concerning the evaluation of saturation fluid temperature. The differences between initially-charged and measured local compositions are significant especially for higher vapour mass fractions as given in Niederkrüger, Steiner et al. [23]. Using the boiling-diagram or equation of state, the error in the saturation temperature can be estimated and reaches values between 0.5 and 1 K. Depending on the mixture used this error might be unacceptable if the measured heat transfer data belong to the convective evaporation region. Therefore, it can be concluded that the measurement technique is doubtful in many experiments.

As wide-boiling mixtures result in heat transfer coefficients which are much lower than for single components only the wide-boiling binary mixture C_2F_6/$C_2H_2F_4$ and the ternary mixture C_2F_6/SF_6/$C_2H_2F_4$ has been used as test fluid. In this connection Palen [24] may be cited: “Sometimes what was thought to be fouling was actually a failure to take into account the effects of wide-boiling mixtures on the heat transfer coefficient.”

2. EXPERIMENTS

2.1. Experimental apparatus

A schematic diagram of the test loop is shown in *figure 1*. In the high pressure loop the liquid is recirculated from the storage tank B1 by a hermetically canned motor pump P1. Two calibrated turbine flowmeters, accuracy ±1 % of reading, are installed just before the throttle valve DR. Inlet temperature and pressure are measured to provide the data for an energy balance. The energy balance carried out for heating a pure fluid gives on the average an accuracy of ±3.2 %. All test runs which show no subcooling of the circulating liquid are rejected. The vapour required for the desired vapour mass fraction is

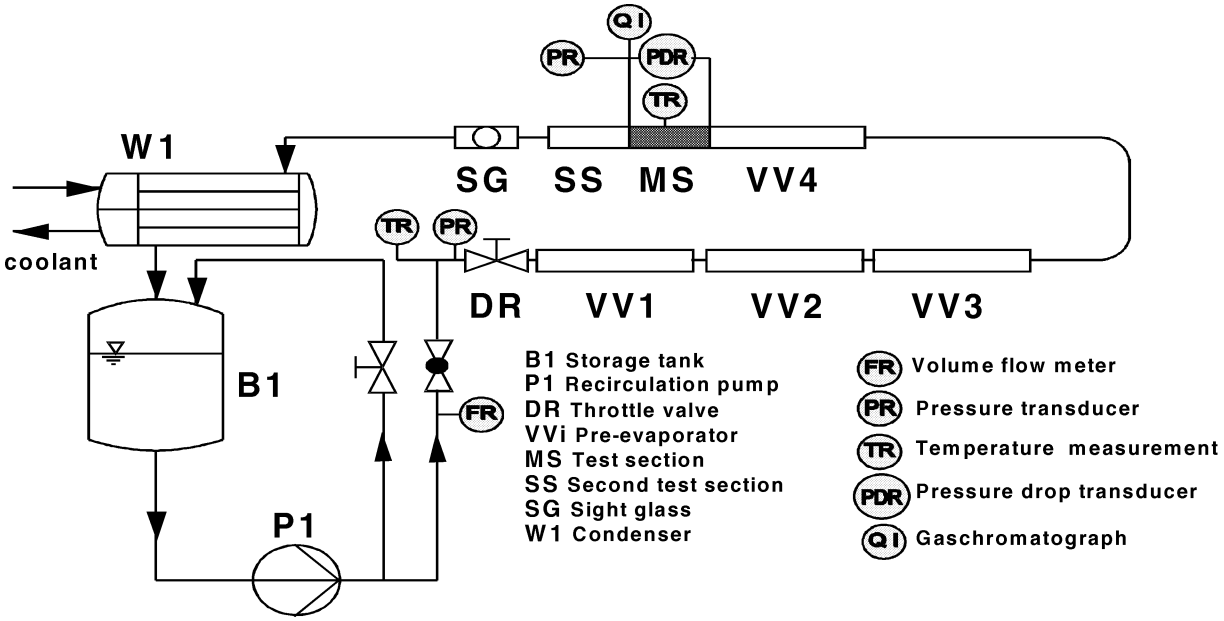

Figure 1. Experimental set-up.

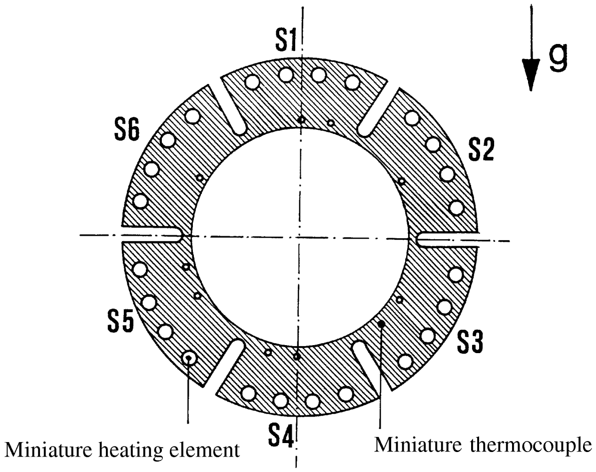

Figure 2. Details of the test section.

generated in four identical pre-evaporators each 1.5 m long (VV1–VV4). The accuracy to determine the vapour mass fraction is within ±4 %.

The test section MS (material nickel) is directly connected to the last pre-evaporator VV4. A second test section SS is used as a thermal guard section. The three units pre-evaporator VV4 and the test sections MS and SS are operated in such a way so as to prevent axial heat conduction and to have a thermally and hydrodynamically developed two-phase flow.

The flow patterns are observed through the glass section SG which is installed after the second test section SS. Finally the vapour generated in the test loop is completely condensed in the condenser W1. A detailed description of the test facility is given by Niederkrüger [25] and Niederkrüger et al. [23].

Local heat transfer coefficients have been obtained by using a test section with six individually heated elements (called S1 to S6) as shown in *figure 2*. In the test section the following quantities are measured: wall temperature with calibrated miniature NiCr–CuNi thermocouples, accuracy ±0.07 K; absolute pressure with a pressure transducer, maximum deviation ±8 mbar; differential pressure with a transmitter, accuracy ±2 % of reading. Additionally, the liquid-phase composition of the flowing mixture is determined by continuously taking very small liquid samples at the inlet and outlet of the test section MS. These samples, average values at the sample position, are completely vaporised and fed into a gas-phase chromatograph by a six-port valve. This technique needs no handling of the samples and therefore involves no material losses. The accuracy of the measured composition is better than ±1 mol%. All tests are recorded when steady-state conditions are reached.

The test series are carried out with decreasing wall superheat starting from the highest selected value to avoid hysteresis effects. According to the local heat transfer process, which mainly depends on the wetting state of the segments (S1 to S6), the power supplied to each of these segments must be varied until a uniform inner wall temperature is achieved.

2.2. Data analysis

Local heat transfer coefficients are determined by using equation (1). The inner wall temperatures, T_W, are calculated from the measured values (distance of thermocouples from inner wall 0.55 mm) by taking into account the temperature drop in the wall (one-dimensional radial, steady-state heat conduction) resulting in corrections usually less than 0.1 K. In equation (1), the temperature of the fluid, T_S, is assumed to be the average thermodynamic equilibrium temperature. Therefore, for the pure components of the mixtures, T_S is the saturation temperature at static pressure, determined from the measured pressure at the test section outlet and the pressure drop assuming a linear pressure change along the test section. For mixtures, however, the saturation temperature is measured with the wall temperature in the unheated second test section SS. A comparison with the temperature calculated with an equation of state (Peng–Robinson as modified by Stryjek and Vera [26]), using the measured pressure and composition, shows that the fluid temperatures measured and calculated agree within small deviations.

Heat fluxes, $\dot{q}$, are obtained from the measured heating power and heat gains or losses through the insulation, which are evaluated by measuring the temperature drop in the insulation, and the respective heating surface. The heating power has been measured with precision Wattmeters giving an accuracy of ±1 % of reading. Vapour mass fraction is calculated by an energy balance from the inlet (valve DR) to the test section (plane at position z, where the thermocouples are located) assuming thermodynamic equilibrium.

For each individually heated segment of the test section, a local heat transfer coefficient is defined as

$$\alpha(\varphi, z) = \frac{\dot{q}(\varphi, z)}{T_W(\varphi, z) - T_S(z)} \tag{1}$$

As all experiments are carried out with the boundary condition of uniform wall temperature, the perimeter averaged heat transfer coefficient at the axial position z is given by

$$\bar{\alpha}(z) = \frac{\frac{1}{6}\sum_{i=1}^{6} \dot{q}(\varphi_i, z)}{T_\mathrm{w}(z) - T_\mathrm{s}(z)} \tag{2}$$

The test series make it possible to determine local heat transfer coefficients as well as perimeter averaged values. This is a basis for analysing the effect of two-phase flow, for example flow distribution, wetting behaviour, entrainment, deposition etc., on the heat transfer in horizontal tubes, see Steiner et al. [27].

3. RESULTS AND DISCUSSION

3.1. Mass transfer controlled models

Local (segment 4) heat transfer coefficients of the non-azeotropic binary mixture $C_2F_6/C_2H_2F_4$ are plotted as a function of heat flux for three mass velocities in *figure 3*. In order to compare results with the same test conditions, all other parameters are kept constant as given in the figure. Two regions of heat transfer mechanisms are realized. For the mass velocity $\dot{m} = 400$ kg·m^{-2}·s^{-1} the region of forced convective evaporation is dominant. In contrast to this result, the tests with the mass velocity of 80 kg·m^{-2}·s^{-1} show the region of nucleate flow boiling for heat fluxes higher than 20 kW·m^{-2}. This confirms well established results for pure fluids as given by Steiner [28].

In *figure 4* local heat transfer coefficients at 11 bar pressure, a vapour mass fraction of 0.5 and a mass velocity of 400 kg·m^{-2}·s^{-1} are plotted as a function of the local liquid phase composition of C_2F_6. The following main results can be concluded from this figure. First, the data determined to a heat flux of 1.5 kW·m^{-2} correspond to the convective evaporation region. In this region the heat transfer coefficients can be evaluated with a correlation derived for pure fluids, but using physical properties of the mixture. An additional mass transfer effect can be neglected. This agrees, for example, with findings of Jain and Dhar [7], Jung et al. [10] and Steiner [29] and has been confirmed by Gropp [30] with experiments of evaporation of falling films. In contrast with these results the heat transfer data of Palen [31] in falling film evaporation with high viscous water/1,2-propylene glycol mixtures showed a significant reduction of measured heat transfer coefficients compared to the evaluated ones using an ideal mixing rule with two pure component coefficients. However, an analysis of Numrich [32] showed that these heat transfer data can be predicted without considering mass transfer effects, when a reliable heat transfer correlation with the Reynolds and Prandtl numbers of the film are taken into account. In this correlation physical properties of the mixture have to be used. Second, the experimental data to the heat flux of 69 kW·m^{-2} show a high reduction of mixture heat transfer depending on the liquid phase composition. An analysis of the data shows a correlation with the heat flux, therefore the data can be considered to belong to the nucleate flow boiling region. In this region, the reduction of heat transfer cannot be predicted with physical properties of the mixture. An additional parameter is needed which is called the mixture flow boiling correction factor. This factor is based on three groups of models. These are the empirical models, e.g., Jung et al. [11], the thermodynamically based models of Stephan and Körner [33] and Murata and Hashizume [34] using the excess wall superheat and the

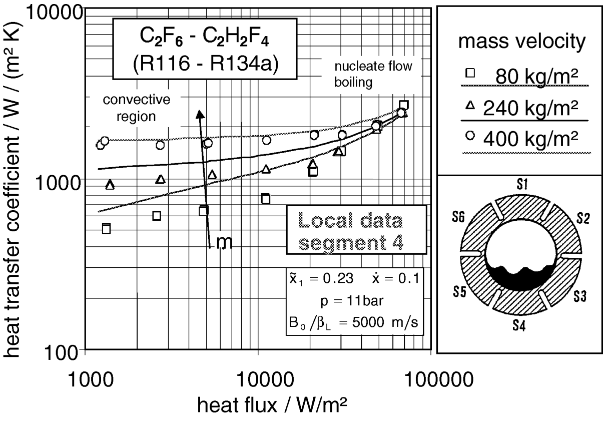

Figure 3. Heat transfer coefficient as a function of heat flux. Mixture $C_2F_6/C_2H_2F_4$ with a local liquid phase composition of 23 mol% C_2F_6.

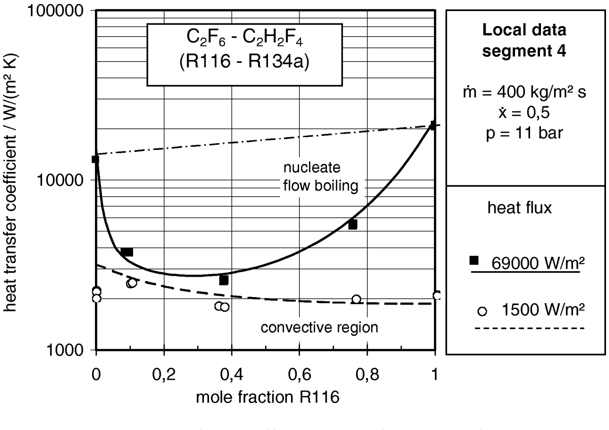

Figure 4. Heat transfer coefficient as a function of liquid phase composition.

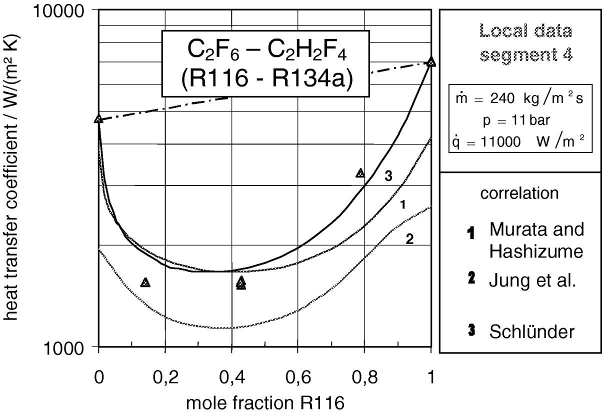

Figure 5. Comparison of predicted and experimental heat transfer coefficients. Vapour mass fraction $\dot{x} = 0.3$.

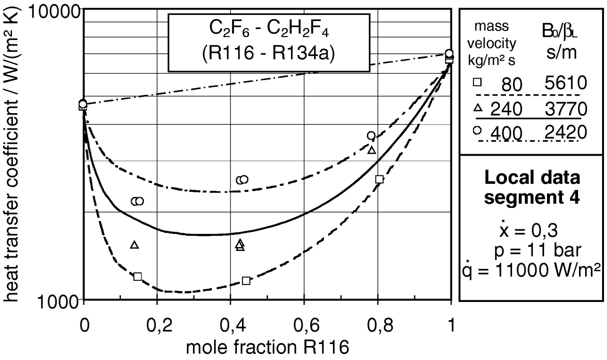

Figure 6. Effect of mass velocity on the mixture heat transfer coefficient.

mass transfer controlled models as given, for example, by Calus et al. [2], Bennett and Chen [5], Schlünder [14] and Thome [13]. A comparison of predicted data using the correlations given by Murata and Hashizume [34], Jung et al. [11] and Schlünder [14] with experimental data is shown in *figure 5*. There is not only a deviation from predicted pure substance heat transfer coefficients, but there are also considerable differences in the mixture region. These can be detected, if the ratio of predicted pure substance heat transfer coefficients to measured ones is normalized to unity.

In the following this nucleate flow boiling region will be discussed only. From *figure 6* can be concluded that the heat transfer coefficient in the middle region of liquid phase composition is significantly affected by the mass velocity. This is due to two main effects. One effect results from the low contribution of the nucleate boiling mechanism on heat transfer. Therefore, the contribution of the convective evaporation to heat transfer is of the same order of magnitude. The second effect results from the direct effect of the liquid phase velocity on the mass transfer coefficient which increases, if the velocity of liquid phase is also increasing. This happens, when the mass velocity and/or the vapour mass fraction is increased. In *figure 6*, the mass transfer coefficient of liquid phase is indicated as β_{L}. The importance of the parameter B_0/β_{L} is explained below.

3.2. Heat transfer of mixtures

On the basis of the previously mentioned results, the heat transfer coefficient can be modelled using the equations given by Steiner [29] in the VDI-Wärmeatlas, as long as the high heat flux boundary is not exceeded.

Region of convective evaporation. The heat flux is lower than the heat flux for the onset of nucleate boiling.

$$\dot{q} < \dot{q}_{\mathrm{ONB}} \quad (\dot{q}_{\mathrm{ONB}} \text{ see equation (6)}) \tag{3}$$

resulting in the heat transfer coefficient

$$\alpha_{\mathrm{cv}} = \alpha_{\mathrm{ce}} \tag{4}$$

with

$$\alpha_{\mathrm{ce}} = \alpha_{\mathrm{L0}} \left\{ (1-\dot{x})^{0.01} \left[(1-\dot{x}) + 1.2\dot{x}^{0.4} \left(\frac{\rho_{\mathrm{L}}}{\rho_{\mathrm{G}}} \right)^{0.37} \right]^{-2.2} + \dot{x}^{0.01} \left[\frac{\alpha_{\mathrm{G0}}}{\alpha_{\mathrm{L0}}} \left(1 + 8(1-\dot{x})^{0.7} \cdot \left(\frac{\rho_{\mathrm{L}}}{\rho_{\mathrm{G}}} \right)^{0.67} \right) \right]^{-2} \right\}^{-0.5} \tag{5}$$

In equation (5) α_{L0} and α_{G0} are the local convective heat transfer coefficients based on the total mass velocity assumed as liquid (L0) or vapour (G0). Standard equations from the literature for tube-side convective heat transfer can be used. All physical properties are mixture properties.

Region of nucleate flow boiling. The heat flux for onset of nucleate boiling is given as

$$\dot{q}_{\mathrm{ONB}} = \frac{2T_{\mathrm{s}}\sigma\alpha_{\mathrm{L0}}}{r_{\mathrm{cr}}\tilde{\rho}_{\mathrm{G}}\Delta\tilde{h}_{\mathrm{v}}} \tag{6}$$

The critical radius $r_{\mathrm{cr}} = 3 \cdot 10^{-6}$ m is to be used. If the heat flux exceeds the value for onset of nucleate boiling

$$\dot{q} \geq \dot{q}_{\mathrm{ONB}} \tag{7}$$

the total heat transfer coefficient can be written as

$$\alpha_{\mathrm{cv}} = \left(\alpha_{\mathrm{ce}}^3 + \alpha_{\mathrm{nbf}}^3 \right)^{1/3} \tag{8}$$

In equation (8) α_{nbf} is the nucleate flow boiling heat transfer coefficient

$$\alpha_{\text{nbf}} = \frac{\alpha_{\text{id}}}{1 + \frac{\alpha_{\text{id}}}{\dot{q}} \Delta T_{\text{bp}} \left[1 - \exp\left(-\frac{B_0}{\beta_{\text{L}}} \cdot \frac{\dot{q}}{\tilde{\rho}_{\text{L}} \Delta \tilde{h}_{\text{v}}}\right)\right]} \tag{9}$$

For mixtures without azeotropes the linear molar mixing law gives the ideal heat transfer coefficient (mixture with K components)

$$\frac{1}{\alpha_{\text{id}}} = \sum_{j=1}^{K} \frac{\tilde{x}_j}{\alpha_{\text{nbf},j}} \tag{10}$$

Since the azeotrope mixture behaves as pure fluid, equation (10) must be modified with mixture compositions of the azeotropes, see Schlünder [14]. In equation (10) $\alpha_{\text{nbf},j}$ are the nucleate flow boiling heat transfer coefficients of the pure components respectively the azeotrope mixtures, as given by Steiner [29]. The physical properties in equations (6) and (9) are mixture properties.

The following correlation is to be used to predict the parameter B_0/β_{L}:

$$\frac{B_0}{\beta_{\text{L}}} \cdot \frac{\alpha_{\text{id}}}{c_{\text{pL}} \rho_{\text{L}}} = 40.6 \left(\frac{\dot{q}}{\dot{q}_0}\right)^{1.19} \left(\frac{\dot{m}}{\dot{m}_0}\right)^{-0.77} \dot{x}^{-0.15} \tag{11}$$

with the reference values $\dot{q} = 20\,000$ W·m^{-2}; $\dot{m}_0 = 100$ kg·m^{-2}·s^{-1}.

The available data bank with 1 351 test runs of the mixture $C_2F_6/C_2H_2F_4$ was used to adjust the constant and exponents in equation (11). The predictive method has been compared with the experimental data and results in a mean relative deviation of 16 %. The performance of the proposed method was evaluated with 593 test runs of the mixture SF_6/CCl_2F_2. The results show a mean relative deviation of 15.1 %. The data of the ternary mixture $C_2F_6/SF_6/C_2H_2F_4$ with 168 test runs can be predicted with a mean relative deviation of 12.4 %.

3.3. Boundary of mass transfer controlled nucleate flow boiling

Today experimental data are not available which do show the heat transfer characteristics of mixtures when high-performance vaporizers must be designed. These vaporizers are operated with high heat fluxes, but not exceeding the critical heat flux. *Figure 7* shows the experimental results for a heat flux of $\dot{q} = 69$ kW·m^{-2}.

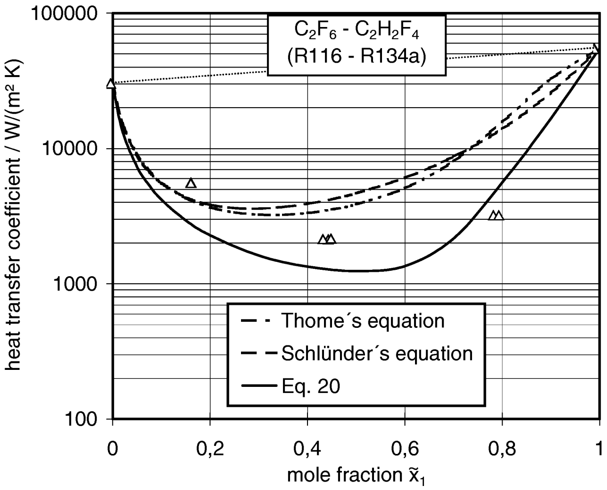

Figure 7. Degradation of experimental heat transfer coefficients of S4 compared with predicted ones as a function of liquid phase composition. Mass velocity 240 kg·m^{-2}·s^{-1}, vapour mass fraction 0.3, pressure 27 bar, heat flux 69 kW·m^{-2}.

For liquid phase compositions higher than 0.4, considerable deviations occur between experimental and predicted heat transfer coefficients, using the mass transfer controlled equations of Section 3.1. A better approximation, however, cannot be obtained when the parameter B_0/β_{L} of the mass transfer controlled model is adjusted to any value in the set of positive real numbers. To analyse the reason of the obtained deviation, equation (9) of Schlünder [14], in the modification of Thome [13], has been rearranged in the form of the mass transfer function

$$\exp\left(-\frac{B_0}{\beta_{\text{L}}} \cdot \frac{\dot{q}}{\tilde{\rho}_{\text{L}} \Delta \tilde{h}_{\text{v}}}\right) = 1 - \frac{\dot{q}(\alpha_{\text{id}}/\alpha_{\text{nbf}} - 1)}{\alpha_{\text{id}} \Delta T_{\text{bp}}} \tag{12}$$

For positive real numbers the left-hand side of equation (12) is only defined in the region from 0 to 1. Using the experimentally determined values, heat flux, $\dot{q}$, heat transfer coefficient, α_{nbf}, the predicted values of boiling range, ΔT_{bp}, and ideal heat transfer coefficient, α_{id}, of the corresponding data set, the right-hand side can be calculated. The result for one run of experiments is given in *figure 8*. For high heat fluxes of more than 40 kW·m^{-2}, the experiments result in negative values, which cannot be admitted for the left-hand side function. This means the mass transfer based model of mixture heat transfer cannot be extended to high heat flux conditions.

The analysis of all available data results in a boundary heat flux where the mass transfer function (equation (12)) will be less or equal to zero. The data base includes

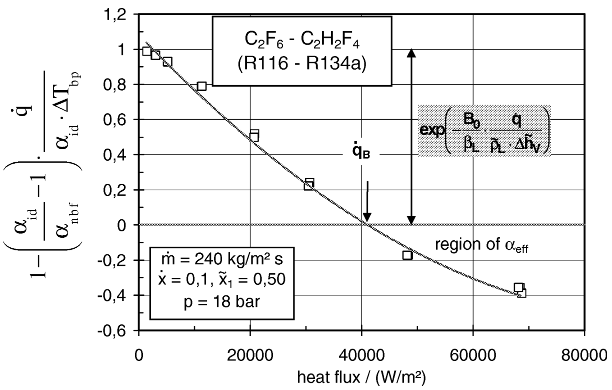

Figure 8. Dependence of mass transfer function, equation (12), on the heat flux.

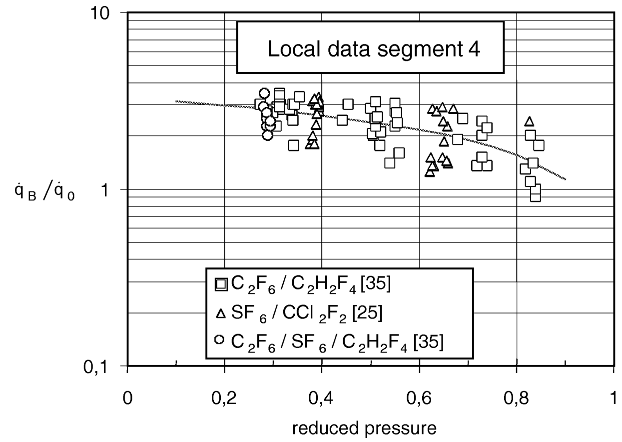

Figure 9. Boundary heat flux as a function of reduced pressure.

the binary mixtures $C_2F_6/C_2H_2F_4$ and SF_6/CCl_2F_2 and the ternary mixture $C_2F_6/SF_6/C_2H_2F_4$, in total 294 test runs. These data show that the boundary heat flux, $\dot{q}_B$, is affected by the reduced pressure as plotted in *figure 9*. An effect of the other parameters could not be ascertained. The following equation is determined by curve fit from the data:

$$\frac{\dot{q}_B}{\dot{q}_0} = 3.3(1 - p_r)^{0.47} \tag{13}$$

In this equation, $\dot{q}_0$ is the reference value $\dot{q}_0 = 20\,000\ \mathrm{W{\cdot}m^{-2}}$.

The reduced pressure $p_r = p/p_{c,m}$ has to be determined from a linear mole fraction weighting of the pure component critical pressure values $p_{c,j}$ as

$$p_{c,m} = \sum_{j=1}^{K} \tilde{x}_j p_{c,j} \tag{14}$$

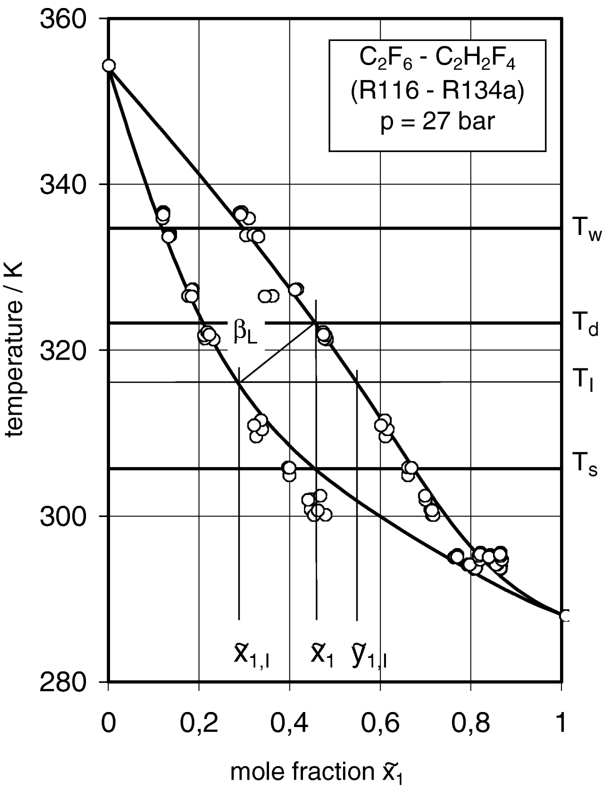

Figure 10. Temperature-composition diagram. Experimental data and prediction with the PRSV2 equation of state [26].

As an increasing number of high-performance heat exchangers with vaporization must be designed, the heat transfer coefficient for the high heat flux region must be known. Calus et al. [2] assumed that for the boiling process the effective temperature difference

$$\Delta T_{eff} = T_w - T_I \tag{15}$$

is responsible as driving force, see *figure 10*. The temperature at the liquid–vapour interphase of the bubbles, T_I, depends dominantly on the mass transfer coefficient of the liquid phase, see Schlünder [14]. If the mass transfer coefficient, β_L, becomes infinite, no difference between the composition of the liquid bulk and the interphase exists and $T_I = T_s(\tilde{x}_1)$. However, for each finite mass transfer coefficient, the temperature T_I rises because the less volatile component is enriched within the boundary layer (interphase).

Schlünder [14] assumed that α_{id} from equation (10) may be taken as the heat transfer coefficient acting with the driving force $(T_w - T_I)$:

$$\dot{q} = \alpha_{id}(T_w - T_I) \tag{16}$$

The evaluation of experiments carried out at the same heat flux and other conditions results in

$$\dot{q} = \alpha_{\mathrm{nbf}}(T_{\mathrm{w}} - T_{\mathrm{s}}) \tag{17}$$

where T_{s} is the saturation temperature to bulk conditions $(\tilde{x}_1, \tilde{x}_2, \ldots, \tilde{x}_{K-1}, p)$.

The maximum interphase temperature can be reached, if the bulk liquid at the composition $\tilde{x}_1$ is local total vaporized, this means the vapour leaves with the local vapour composition $\tilde{y}_{1\mathrm{I}} = \tilde{x}_1$, see *figure 10*. This is possible for high heat fluxes. Then, the interphase temperature T_{I} will reach the dew temperature T_{d}.

Assuming $T_{\mathrm{I}} = T_{\mathrm{d}}$ the heat transfer coefficient α_{eff} may be defined by

$$\dot{q} = \alpha_{\mathrm{eff}}(T_{\mathrm{w}} - T_{\mathrm{d}}) \tag{18}$$

Using the experimentally determined heat transfer coefficient, α_{nbf}, the combination of equations (17) and (18) yields:

$$\alpha_{\mathrm{eff}} = \frac{\alpha_{\mathrm{nbf}}}{1 - (\alpha_{\mathrm{nbf}}/\dot{q})(T_{\mathrm{d}} - T_{\mathrm{s}})} \tag{19}$$

This “effective” heat transfer coefficient can be correlated from the previously cited 294 test runs with the binary mixtures $C_2F_6/C_2H_2F_4$ and SF_6/CCl_2F_2 and the ternary mixture $C_2F_6/SF_6/C_2H_2F_4$. As result one gets

$$\frac{\alpha_{\mathrm{eff}}}{\alpha_{\mathrm{id}}} = \left[1 - 0.25\left(\frac{\dot{q}}{\dot{q}^*_{\mathrm{cr,nb}}}\right)^{1.5}\right]^{215\Delta T_{\mathrm{bp}}/(T_{\mathrm{c,max}} - T_{\mathrm{c,min}})} \tag{20}$$

Here, $T_{\mathrm{c,max}}$ is the highest critical temperature and $T_{\mathrm{c,min}}$ is the lowest critical temperature of any pure component in the mixture. From the experimental data, equation (20) could be verified in the range $T_{\mathrm{c,max}} - T_{\mathrm{c,min}} = 81.2$ K. The ideal heat transfer coefficient is given by equation (10). The heat flux $\dot{q}_{\mathrm{cr,nb}}$, as given in [29], is a reference value and to be calculated as

$$\dot{q}_{\mathrm{cr,nb}} = 0.13\Delta h_{\mathrm{v}}\rho_{\mathrm{G}}^{0.5}\left(\sigma g(\rho_{\mathrm{L}} - \rho_{\mathrm{G}})\right)^{0.25} \tag{21}$$

with mixture properties at the given pressure. In equation (20) $\dot{q}^*_{\mathrm{cr,nb}}$ is to calculate as

$$\dot{q}^*_{\mathrm{cr,nb}} = 2.79\dot{q}_{\mathrm{cr,nb}}p_{\mathrm{r}}^{0.4}(1 - p_{\mathrm{r}}) \tag{22}$$

(see reference [29]). The reduced pressure is to estimate from equation (14).

For high heat fluxes the term in the brackets of the denominator of equation (9) converge to unity. So, the contribution of nucleate flow boiling to the heat transfer for heat fluxes higher than the boundary heat flux, $\dot{q}_{\mathrm{B}}$, is given as

$$\frac{\alpha_{\mathrm{nbf}}}{\alpha_{\mathrm{eff}}} = \left[1 + \frac{\alpha_{\mathrm{eff}}}{\dot{q}}\,\Delta T_{\mathrm{bp}}\right]^{-1} \tag{23}$$

In all cases, the convective contribution to the heat transfer has to be predicted with equation (5). The total heat transfer coefficient is determined by

$$\alpha_{\mathrm{cv}} = \left(\alpha_{\mathrm{ce}}^3 + \alpha_{\mathrm{nbf}}^3\right)^{1/3} \tag{24}$$

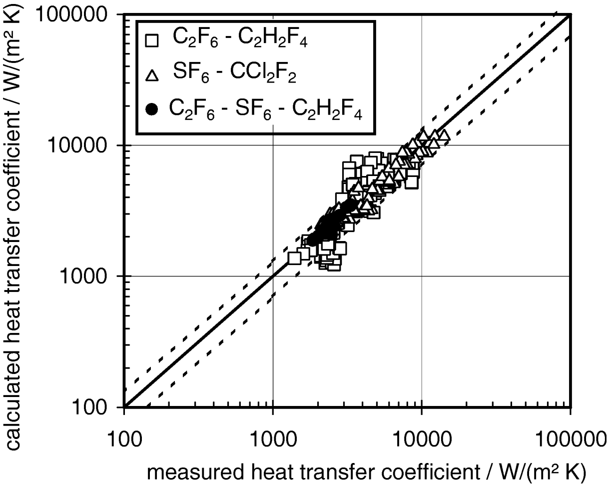

Figure 11. Prediction of 294 data points by the proposed method, Section 3.3, for the high heat flux region.

For comparison, experimental data of the binary mixtures $C_2F_6/C_2H_2F_4$ and SF_6/CCl_2F_2 and the ternary mixture $C_2F_6/SF_6/C_2H_2F_4$ were evaluated with equation (24). The result of the available 294 data points is shown in *figure 11*. The measured heat transfer coefficients can be predicted with a mean relative deviation of 15 %. Additionally, the ±30 % range of deviation is plotted in this figure.

The curve from equation (24) is plotted in *figure 7* to show the effect of the proposed method of Section 3.3 in comparison with the experimental data. Especially the data with mole fractions larger than 0.4 are quite better predicted.

3.4. Conclusions

An experimental study of flow boiling heat transfer with the wide-boiling binary mixture of $C_2F_6/C_2H_2F_4$ and of the ternary mixture $C_2F_6/SF_6/C_2H_2F_4$ has been carried out. These mixtures are non-azeotropic mixtures with a difference in boiling points of 52 K at the pressure of 1 bar. The condition of uniform inner wall temperature at the tube perimeter has been used during the heat transfer experiments in the horizontal test section. Only the heat transfer coefficient for the fully-wetted bottom segment (S4) have been reported. Therefore, the results can also be considered as representative for the heat transfer in vertical tubes. The deviation of these local data from data obtained in a vertical tube falls within the experimental accuracy.

The heat transfer tests show the regions of forced convective evaporation and of nucleate flow boiling. The dominance of one region or the other depends on the experimental parameters. In the convective evaporation region the heat transfer coefficients are lower than the values calculated by the ideal mixing rule. However, the experimental data can be predicted with a pure fluid correlation taking into account physical mixture properties alone. In the nucleate flow boiling region a considerable decrease of heat transfer coefficients occurs when compared with the values calculated by the ideal mixing rule. In a large range of parameters this degradation can be predicted by the mass transfer controlled models of Schlünder [14] or Thome [13]. The basis of these correlations is the ideal heat transfer coefficient always predicted with nucleate flow boiling heat transfer coefficients of the pure mixture components.

In the parameter region of high heat fluxes (high-performance region) the mass transfer controlled model can only explain a part of the heat transfer degradation because the heat transfer coefficients are much lower than those predicted from any mass transfer controlled model. Therefore, a model of an “effective” heat transfer coefficient must be used as the basis, instead of the previously applied ideal heat transfer coefficient.

Acknowledgements

The authors gratefully acknowledge the financial support for this work by the Deutsche Forschungsgemeinschaft (DFG), Bonn-Bad Godesberg.

The authors thank Mr. Markus Nickolay for the help in the design of the figures.

REFERENCES

[1] Palen J.W., Small W., A new way to design kettle and internal reboilers, Hydrocarbon Process 43 (11) (1964) 199–208.

[2] Calus W.F., di Montegnacco A., Denning R.K., Heat transfer in a natural circulation single tube reboiler. Part II: Binary liquid mixtures, Chem. Engrg. J. 6 (1973) 251–264.

[3] Shock R.A.W., The evaporation of binary mixtures in forced convection, Ph.D. Thesis, University of Oxford, Oxford, 1973.

[4] Zizyukin V.K., Aérov M.É., Heat transfer to certain boiling hydrocarbons during their forced motion in a horizontal tube, Theoret. Khimi. Tekhnologii 9 (1) (1975) 54–59.

[5] Bennett D.L., Chen J.C., Forced convective boiling in vertical tubes for saturated pure components and binary mixtures, AIChE J. 26 (3) (1980) 454–461.

[6] Toral H., Kenning D.B.R., Shock R.A.W., Flow boiling of ethanol/cyclohexane mixtures, in: Proc. 7th Int. Heat Transfer Conf., München, Vol. 4, 1982, 255–260.

[7] Jain V.K., Dhar P.L., Studies on flow boiling of mixtures of refrigerants R12 and R13 inside a horizontal tube, in: Proc. XVIth Int. Congr. Refrig., Paris, Vol. B1, 1983, 287–292.

[8] Radermacher R., Ross H., Didion D., Experimental determination of forced convection evaporative heat transfer coefficients for non-azeotropic refrigerant mixtures, in: ASME Nat. Heat Transfer Conf., ASME Paper No. 83-WA/HT 54, 1983.

[9] Ross H., Radermacher R., di Marzo M., Horizontal flow boiling of pure and mixed refrigerants, Int. J. Heat Mass Tran. 30 (5) (1987) 979–992.

[10] Jung D.S., McLinden M., Radermacher R., Didion D., Horizontal flow boiling heat transfer experiments with a mixture of R22/R114, Int. J. Heat Mass Tran. 32 (1) (1989) 131–145.

[11] Jung D.S., Radermacher R., Prediction of evaporation heat transfer coefficient and pressure drop of refrigerant mixtures, Int. J. Refrig. 16 (5) (1993) 330–338.

[12] Chen J.C., A correlation for boiling heat transfer to saturated fluids in convective flow, in: ASME Nat. Heat Transfer Conf., ASME Paper No. 63-HT-34, Boston, 1963, 1–11.

[13] Thome J.R., Prediction of the mixture effect on boiling in vertical thermosyphon reboilers, Heat Transfer Engrg. 10 (2) (1989) 29–38.

[14] Schlünder E.-U., Über den Wärmeübergang bei der Blasenverdampfung von Gemischen, vt Verfahrenstechnik 16 (9) (1982) 692–698.

[15] Hihara E., Saito T., Forced convective boiling heat transfer of binary mixtures in a horizontal tube, in: Proc. 9th Int. Heat Transfer Conf., Jerusalem, Vol. 1-BO-21, 1990, 123–128.

[16] Hihara E., Saito T., Boiling heat transfer of mixed refrigerants inside horizontal smooth tubes, in: Proc. 2nd Japanese–German Symposium on Multi-Phase Flow, No. 1-5-3, 1997, 189–196.

[17] Takamatsu H., Miyara A. Koyama S., Fujii T., Yonemoto K., Forced convective boiling of non-azeotropic refrigerant mixtures of R22 and R114 inside a horizontal tube, Heat Transfer Jpn. Res. 19 (3) (1990) 68–82.

[18] Celata G.P., Cumo M., Setaro T., Forced convective boiling in binary mixtures, Int. J. Heat Mass Tran. 36 (13) (1993) 3299–3309.

[19] Celata G.P., Cumo M., Setaro T., Vertical forced convective boiling of refrigerant binary mixtures, Rev. Gén. Therm. 36 (1997) 253–263.

[20] Fujita Y., Tsutsui M., Convective flow boiling of binary mixtures in a vertical tube, in: Convective Flow Boiling, Taylor & Francis, Washington, 1996, 259–264.

[21] Melin P., Vamling L., Flow boiling heat transfer and pressure drop for zeotropic mixtures in a horizontal tube, in: Proc. Int. Symp. Two-Phase Flow Modelling and Experimentation, Rome, 1995, 1–23.

[22] Aprea C., Betta V., Greco A., Mastrullo R., Experimental comparison of R22 and R407C heat transfer coefficients, in: Proc. Int. Conf. Heat Exchangers for Sustainable Development, Lisbon, 1998, 653–664.

[23] Niederkrüger M., Steiner D., Schlünder E.-U., Horizontal flow boiling experiments of saturated pure components and mixture of R846–R12 at high pressures, Int. J. Refrig. 15 (1) (1992) 48–58.

[24] Palen J.W., Shell-and-tube reboilers, in: Heat Exchanger Design Handbook (HEDH), Section 3.6.1, Introduction, Begell House, Inc., New York, 1997.

[25] Niederkrüger M., Strömungssieden von reinen Stoffen und binären zeotropen Gemischen im waagerechten Rohr bei mittleren und hohen Drücken, Diss., Univ. Karlsruhe, in: Fortschritt-Berichte VDI, Reihe 3, No. 245, Düsseldorf, 1991.

[26] Stryjek R., Vera J.H., PRSV2: A cubic equation of state for accurate vapour–liquid equilibria calculations, Canadian J. Chem. Engrg. 64 (1986) 820–826.

[27] Steiner D., Wettermann M., Interaction of vapour-liquid two-phase flow and heat transfer in a horizontal tube, in: Proc. Int. Eng. Found. Conf. Convective Flow and Pool Boiling, Irsee, Ses. VI, 1997, 1–8.

[28] Steiner D., Wärmeübertragung beim Sieden gesättigter Flüssigkeiten, in: VDI-Wärmeatlas, Section Hbb, 4. Auflage, VDI-Verlag, Düsseldorf, 1984.

[29] Steiner D., Wärmeübertragung beim Sieden gesättigter Flüssigkeiten, in: VDI-Wärmeatlas, Section Hbb, 6. Auflage, VDI-Verlag, Düsseldorf, 1991.

[30] Gropp U., Wärme- und Stoffübergang bei der Oberflächenverdampfung und beim Blasensieden eines binären Kältemittelgemisches am Rieselfilm, Diss., Univ. Karlsruhe, 1985.

[31] Palen J.W., Falling film evaporation of wide-boiling-range mixtures inside a vertical tube, Ph.D. Diss., Lehigh Univ., U.M.I. No. 8817485, 1988.

[32] Numrich R., Falling film evaporation of soluble mixtures, in: Convective Flow Boiling, Taylor & Francis, Washington, 1996, 335–338.

[33] Stephan K., Körner M., Berechnung des Wärmeübergangs verdampfender binärer Flüssigkeitsgemische, Chem.-Ing.-Tech. 41 (1969) 409–417.

[34] Murata K., Hashizume K., An investigation of forced convection boiling of nonazetropic refrigerant mixtures, Heat Transfer Jpn. Res. 19 (1990) 95–109.

[35] Wettermann M., Wärmeübergang beim Sieden von Gemischen bei Zwangskonvektion im horizontalen Verdampferrohr, Diss., Univ. Karlsruhe, 1999.